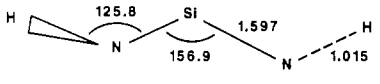

dihedral HNSiN = ±141.5

Figure 2. MP2/6-31G(d) structure for siladiimide. Bond lengths are in Å; angles are in deg.

Table II. Potential Energy Surface (kcal/mol) for HNSiNH[a]

	energy for dihedral angle					
HNSi angle	180°	160°	140°	120°	100°	90°
180	0.2	0.2	0.2	0.2	0.2	0.2
170	0.1	0.1	0.2	0.2	0.3	0.3
160	0.0	0.1	0.2	0.4	0.6	0.8
150	0.1	0.2	0.3	0.6	1.1	1.3
140	0.8	0.8	0.9	1.1	1.6	2.0
130	2.5	2.4	2.2	2.2	2.6	2.9
120	5.7	5.5	4.9	4.4	4.3	4.6
110	11.0	10.5	9.4	8.3	7.7	7.8
100	18.4	17.8	16.2	14.6	13.6	13.5

[a] Angles in degrees.

the nitrogens in the nitrogen lone pairs increases to 1.829 when **2** is rotated to a structure with a bond angle of 120° and a dihedral angle of 90°.

The rather small energy difference between planar and linear siladiimide is suggestive of a very flat conformational potential energy surface in this molecule. To investigate this further, the SiN and NH bond lengths were reoptimized as a function of the HNSi bond angle and the HNNH dihedral angle, maintaining the linearity of the NSiN angle. The results of these calculations are displayed in Table II, where the energy (relative to the global minimum) is given as a function of the HNSi angle for several values of the dihedral angle ranging from 90 to 180°. As expected, a large portion of the surface is very flat. For each value of the dihedral angle the energy variation is less than 3 kcal/mol for angles between 130 and 180°. Viewed in another manner, for angles from 120 to 180°, the energy variation is less than 1 kcal/mol for the full range of dihedral angles investigated. Note that for bond angles between 140 and 180° the lowest energy geometry is planar, whereas for bond angles below 140° the orthogonal structure is preferred. Thus, in this compound there appears to be an almost equal balance between π-bond energies (favoring the traditional allenic structure) and nitrogen lone-pair delocalization (favoring a planar structure).

The extremely flat potential energy surface for siladiimide suggests that correlation corrections to the energy might play an important role. Thus, the structure of this molecule was fully reoptimized with MP2/6-31G(d) wave functions in C_2 symmetry. The final structure, verified as a minimum by diagonalizing the matrix of energy second derivatives, is displayed in Figure 2. In contrast to the SCF structures, the molecule is found to have a nonlinear N=Si=N angle, with noncoplanar hydrogens, at the MP2 level of theory. For completeness, the SCF structure was reoptimized in C_2 symmetry, starting from the MP2 geometry, and the NSiN bond returns to linearity. So, the bending of this angle is a correlation effect. A similar effect has been observed for propadienone.[14]

The structure shown in Figure 2 is 2.1 kcal/mol below that optimized with a NSiN angle constrained to 180°. Higher level computations have only a small effect on this energy difference. At the MP2/6-31G(d) optimized geometries, MP4/6-31G(d,p) calculations increase the relative stability of the twisted structure (Figure 2) to 3.1 kcal/mol. Thus, even though the potential energy surface remains very flat (and therefore the foregoing qualitative analysis of the SCF structural preferences probably remain valid), introduction of correlation corrections produces a nonplanar structure more in keeping with that of allene, albeit with a nonlinear N=Si=N moiety.

It is interesting that the semiempirical calculations performed by Welsh and co-workers[6b] on the *N,N*-dimethylated structure has some resemblance to that shown in Figure 2, with a dihedral angle of 3° and an NSiN angle of 172°.

In conclusion, our calculations indicate that this species may adopt a classical allene-like structure (although with a nonlinear NSiN angle) or a trans planar structure. There is very little energy difference between these, so it seems likely that crystal packing forces will play a large role in determining the structure of substituted diimides in the solid state.

Acknowledgment. We are indebted to Professor Josef Michl for several useful discussions regarding this problem. The work reported here was supported in part by grants from the Air Force Office of Scientific Research (87-0049) and the National Science Foundation (CHE86-40771). The computer time made available by the North Dakota State University Computer Center is gratefully acknowledged.

Contribution from the Faculty of Pharmaceutical Sciences, Nagoya City University, Mizuho-ku, Nagoya 467, Japan

Low-Spin Tetracyanoferrate(II) and -(III) Complexes of Meso-Type 1,2-Diamines: Synthesis and Steric Effects on Chelate-Ring Conformation and Rate of Ligand Dehydrogenation

Yoshitaka Kuroda, Noriko Tanaka, Masafumi Goto,* and Tomoya Sakai

Received December 11, 1987

Tetracyano(1,2-diamine)ferrate(II) and -(III) complexes were synthesized by using (1*R*,2*S*)-*cis*-cyclohexanediamine (*cis*-chxn), (2*R*,3*S*)-butanediamine (*meso*-bn), and (2*R*,3*R*)-butanediamine (*R*-bn) as 1,2-diamines. ^{1}H and ^{13}C NMR spectra confirmed that the *cis*-chxn and *meso*-bn complexes alternated their chelate-ring conformations from δ to λ rapidly on the NMR time scale in solution at room temperature, while the *R*-bn complex assumed a predominantly λ conformation. The oxidation product of the *meso*-bn complex, tetracyano(2,3-butanediimine)ferrate(II), was isolated and characterized. All Fe^{III} complexes underwent a disproportionation reaction accompanied by diamine dehydrogenation, yielding tetracyanoferrate(II) complexes of diamine, monoimine, and diimine in basic aqueous solutions. The third-order rate constants (M^{-2} s^{-1}) for the disproportionation were as follows: *cis*-chxn, 4.62×10^4; *meso*-bn, 2.34×10^4; *R*-bn, 1.28×10^4. The difference in rate constants is attributed to the strain energy of the chelate ring due to steric repulsion between the axial alkyl group and other protons within the chelate.

Introduction

The chemistry of tetracyano(diamine)ferrate complexes is complex despite their rather simple structure because a redox reaction takes place at the central metal ion (Fe^{II}, **1**; Fe^{III}, **2**) and ligand oxidation also takes place to yield diimine complexes **3**.[1-4] The Fe^{III} complexes (**2**) undergo a disproportionation, yielding **1** and **3**. We have synthesized tetracyanoferrate(II) and tetra-

(1) Goedken, V. L. *Chem. Commun.* **1972**, 207.
(2) Goto, M.; Takeshita, M.; Sakai, T. *Inorg. Chem.* **1978**, *17*, 314.

0020-1669/89/1328-2163$01.50/0

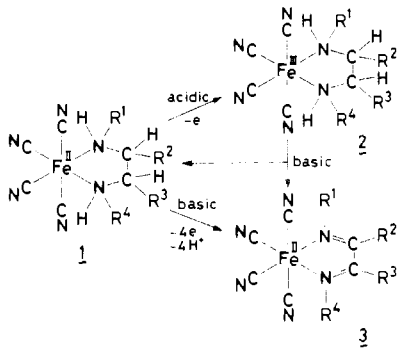

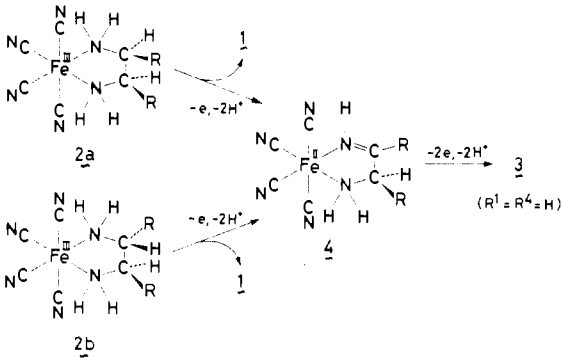

cyanoferrate(III) chelates of two meso-type 1,2-diamines, (2*R*,3*S*)-butanediamine (*meso*-bn) and (1*R*,2*S*)-*cis*-cyclohexanediamine (*cis*-chxn), and one racemic-type 1,2-diamine, (2*R*,3*R*)-butanediamine (*R*-bn), for two reasons, as described below.

The stereochemistry of a 1,2-diamine coordinated to a transition-metal ion is different in racemic- and meso-type 1,2-diamines.[5] Racemic-type 1,2-diamines, such as (1*R*,2*R*)-cyclohexanediamine (*R*-chxn) and *R*-bn, assume a rigid chelate-ring conformation with alkyl group(s) in equatorial positions.[6] On the other hand, the meso-type 1,2-diamines, such as *meso*-bn and *cis*-chxn, form chelate rings in which conformations alternate between δ and λ.[7] We have previously reported ^{1}H and ^{13}C NMR spectra of tetracyanoferrate(II) and tetracyanoferrate(III) complexes of some racemic-type 1,2-diamines.[8] The Fe^{III} complexes gave well-resolved NMR signals, and their shifts were dependent on the orientation of the nuclei relative to the chelate ring. This dependency on orientation can be used to obtain structural information about the diamine chelates. One of the purposes of this work is the elucidation of the difference in the stereochemistry of these racemic- and meso-type 1,2-diamines by ^{1}H and ^{13}C NMR spectroscopy.

Another purpose of this work is to elucidate how the stereochemical differences between the two types of 1,2-diamines reflect the rate and stoichiometry of the disproportionation of **2**. Dehydrogenation of amines coordinated to transition-metal ions is known to occur in Cu,[9] Ni,[9] Ru,[10,11] and Fe[4,12,13] complexes. We have reported[4] that the dehydrogenation of tetracyano(diamine)ferrate(II) (**1**) proceeds in two steps: (i) an oxidation of the central metal ion in **1** to yield **2** and (ii) a base-promoted disproportionation of **2** having the stoichiometry described in eq 1 for the case in which the diamine is *R*-chxn. Results of a kinetic

$$4[Fe^{III}(CN)_4(\text{diamine})]^- + 4OH^- \rightarrow [Fe^{II}(CN)_4(\text{diimine})]^{2-} + 3[Fe^{II}(CN)_4(\text{diamine})]^{2-} + 4H_2O \quad (1)$$

study[4] suggest that the dehydrogenation of **1** to **3** proceeds via the intermediate 2-aminoethanimine (monoimine) **4**. The identical monoimine complex, **4**, can be generated from both the meso- and racemic-type 1,2-diamine complexes **2a** and **2b**. The difference in stereochemistry between these two types of diamines is expected to influence the rate of the first reaction[4,10-13] and has virtually no effect on further reactions subsequent to the formation of the intermediate.

Experimental Section

Materials. (1*R*,2*S*)-*cis*-Cyclohexanediamine was separated from a commercially available mixture of 1,2-cyclohexanediamine (Tokyo Kasei) according to the method of Kidani and Saito.[14] (2*R*,3*S*)-Butanediamine was prepared from dimethylglyoxime by reduction with Raney nickel, as described by Dickey, Fickett, and Lucas.[15] (2*R*,3*R*)-Butanediamine was prepared according to the method of Cooley, Liu, and Bailar[16] and optically resolved by the method of Dickey et al:[15] $[\alpha]^{20}_D$ +17.8° (*c* = 5, water) (lit.[15] $[\alpha]^{25}_D$ +17.8° (*c* = 5, water)). $Na_2[Fe(CN)_4(cis\text{-chxn})]\cdot 2H_2O$ and $Na[Fe(CN)_4(cis\text{-chxn})]\cdot H_2O\cdot 0.5NaClO_4$ were prepared as previously described.[3]

All operations for the preparation of the Fe^{II} complexes were carried out under a nitrogen atmosphere prepurified by being passed successively through an aqueous Cr^{II} solution and sulfuric acid. Oxygen was removed from solvents by bubbling with prepurified nitrogen before use.

CHN analyses were performed at the Elemental Analysis Unit of Nagoya City University.

Preparation of Fe^{II} and Fe^{III} Chelates. $Na_2[Fe(CN)_4(meso\text{-bn})]\cdot 0.5NaClO_4$. $Fe(ClO_4)_2\cdot 6H_2O$ (7.30 g, 0.0201 mol) and 30 mL of methanol were placed in nitrogen-atmosphere-maintained 200-mL round-bottom two-necked flask containing a magnetic stirring bar and equipped with a serum cap and a stopcock. $Fe(ClO_4)_2\cdot 6H_2O$ was dissolved in methanol and cooled in an ice bath. To this was added a methanol solution (15 mL) of *meso*-bn (3.60 g, 0.0408 mol) with stirring, followed by addition of a solution of NaCN (3.96 g, 0.0808 mol) in 20 mL of water with vigorous stirring. After being stirred for 30 min, the reaction mixture was evaporated to near dryness with an aspirator. To the residue was added 50 mL of ethanol, and the mixture was kept at 4 °C overnight. The precipitate was collected on a filter and washed twice with 30 mL of ethanol. The crude product was dissolved in 10 mL of water, and the solution was filtered under nitrogen to remove a small amount of blue precipitate. Ethanol was added to the yellow filtrate until the solution became turbid (80 mL), and the mixture was allowed to stand at 4 °C overnight. A yellow crystalline product was collected on a filter, washed successively with ethanol and ether, and dried in vacuo. Yield: 4.84 g (67.7%). Anal. Calcd for $Na_2[Fe(CN)_4(C_4H_{12}N_2)]\cdot 0.5NaClO_4$: C, 27.05; H, 3.40; N, 23.66. Found: C, 27.27; H, 3.73; N, 23.58.

$Na[Fe(CN)_4(meso\text{-bn})]\cdot 2H_2O$. $Na_2[Fe(CN)_4(meso\text{-bn})]\cdot 0.5NaClO_4$ (1.80 g, 0.00507 mol) was dissolved in a solution of 30% $HClO_4$ (3 mL) and methanol (10 mL) and cooled in an ice-water bath. A 0.65-mL volume of 30% H_2O_2 was added to the solution dropwise with vigorous stirring at 0 °C. Then 18.5 mL of 1-propanol was added, and the resulting mixture was filtered to remove a blue precipitate. Diisopropyl ether was added to the filtrate until the solution became turbid (8 mL), and the mixture was allowed to stand at −15 °C overnight. A yellow crystalline product was collected on a filter, washed with 1-propanol, and dried in vacuo. Yield: 0.720 g (46.3%). Anal. Calcd for $Na[Fe(CN)_4(C_4H_{12}N_2)]\cdot 2H_2O$: C, 31.29; H, 5.25; N, 27.37. Found: C, 31.04; H, 5.22; N, 26.99.

$Na_2[Fe(CN)_4(R\text{-bn})]\cdot 0.5NaClO_4$. A solution of (2*R*,3*R*)-butanediamine (2.40 g, 0.0272 mol) in methanol (10 mL) was added to a solution

(3) Goto, M.; Takeshita, M.; Sakai, T. *Bull. Chem. Soc. Jpn.* **1981**, *54*, 2491.
(4) Goto, M.; Takeshita, M.; Kanda, N.; Sakai, T.; Goedken, V. L. *Inorg. Chem.* **1985**, *24*, 582.
(5) Tapscott, R. E.; Mather, D. J.; Them, T. F. *Coord. Chem. Rev.* **1979**, *29*, 87.
(6) Hawkins, C. J.; Palmer, J. A. *Coord. Chem. Rev.* **1982**, *44*, 1–60.
(7) Hilleary, C. J.; Them, T. F.; Tapscott, R. E. *Inorg. Chem.* **1980**, *19*, 102 and references therein.
(8) Kuroda, Y.; Goto, M.; Sakai, T. *Bull. Chem. Soc. Jpn.* **1987**, *60*, 3917.
(9) Hipp, C. J.; Busch, D. H. In *Coordination Chemistry*; Martell, A. E., Ed.; ACS Monograph 174; American Chemical Society: Washington, DC, 1974; Vol. 2, pp 435.
(10) Ridd, M. J.; Keene, F. R. *J. Am. Chem. Soc.* **1981**, *103*, 5733.
(11) Keene, F. R.; Ridd, M. J.; Snow, M. R. *J. Am. Chem. Soc.* **1983**, *105*, 7075.
(12) Ferreira, A. M. C.; Toma, H. E. *J. Chem. Soc., Dalton Trans.* **1983**, 2051.
(13) Toma, H. E.; Ferreira, A. M. C.; Iha, N. Y. M. *Nouv. J. Chim.* **1985**, *9*, 473.
(14) Saito, R.; Kidani, Y. *Chem. Lett.* **1976**, 123.
(15) Dickey, F. H.; Fickett, W.; Lucas, H. J. *J. Am. Chem. Soc.* **1952**, *74*, 944.
(16) Cooley, W. E.; Liu, C. F.; Bailar, J. C., Jr. *J. Am. Chem. Soc.* **1959**, *81*, 4189.

of $Fe(ClO_4)_2 \cdot 6H_2O$ (4.87 g, 0.0134 mol) in methanol (20 mL) under nitrogen at 0 °C. An aqueous solution (10 mL) of NaCN (2.64 g, 0.0539 mol) was added dropwise to the resulting solution with vigorous stirring at 0 °C. Stirring was then continued for 30 min at this temperature. The mixture was evaporated to near dryness with an aspirator. Cold ethanol (30 mL) was added to the yellow residue, and the mixture was placed at 4 °C overnight. A yellow precipitate was collected on a filter, washed twice successively with ethanol (30 mL) and ether, and dried in vacuo. Yield: 4.70 g (98.6%). The crude product was dissolved in 11 mL of water, and the insoluble materials were filtered off. A 10-mL portion of methanol was added to the filtrate, followed by ethanol until the solution became turbid (80 mL). The resulting mixture was immersed in an ice-water bath, and the white crystalline precipitate that formed was removed by filtration. The filtrate was allowed to stand at −15 °C for 2 h. A yellow crystalline product was collected on a filter, washed twice with 20 mL of ethanol, and dried in vacuo. Yield: 2.98 g (62.5%). Anal. Calcd for $Na_2[Fe(CN)_4(C_4H_{12}N_2)] \cdot 0.5NaClO_4$: C, 27.05; H, 3.40; N, 23.66. Found: C, 26.76; H, 3.86; N, 23.44.

The gravimetric analysis of the perchlorate ion using tetraphenylarsonium chloride–hydrogen chloride accounted for 96.0% of the amount required for the above formula.

Na[Fe(CN)$_4$(*R*-bn)]·2H$_2$O. $Na_2[Fe(CN)_4(R\text{-bn})] \cdot 0.5NaClO_4$ (1.00 g, 2.81 mmol) was dissolved in an ice cold solution of 30% $HClO_4$ (1.5 mL) and ethanol (5 mL). A 0.37-mL volume of 30% H_2O_2 was added dropwise to this solution at 0 °C with vigorous stirring. 1-Propanol (5.5 mL) was then added, followed by diisopropyl ether until the solution became turbid (5.3 mL). The mixture was allowed to stand at −15 °C overnight. A yellow crystalline product was collected on a filter, washed with 1-propanol, and dried in vacuo. Yield: 0.380 g (44.0%). Anal. Calcd for $Na[Fe(CN)_4(C_4H_{12}N_2)] \cdot 2H_2O$: C, 31.29; H, 5.25; N, 27.37. Found: C, 31.34; H, 5.03; N, 27.66.

[C$_8$H$_{18}$N$_2$][Fe(CN)$_4$(2,3-butanediimine)]·2.5H$_2$O. A 5.0-mL volume of 1 M hydrogen peroxide was added dropwise at 40 °C to an aqueous solution of $Na_2[Fe(CN)_4(meso\text{-bn})] \cdot 0.5NaClO_4$ (1 g, 2.82 mmol) in 10 mL of water. The resulting intensely red solution was concentrated on a rotatory evaporator. The red residue was dissolved in 2 mL of water, and 1 g of 1,4-dimethyl-1,4-diazoniabicyclo[2.2.2]octane iodide was added to the solution. Ethanol was added until the solution became turbid, and the mixture was allowed to stand at 4 °C overnight. A red precipitate was collected on a filter and was crystallized from water–ethanol. Anal. Calcd for $[C_8H_{18}N_2][Fe(CN)_4(C_4H_8N_2)] \cdot 2.5H_2O$: C, 44.56; H, 7.24; N, 25.98. Found: C, 44.50; H, 6.80; N, 26.15, ^{1}H NMR: CH_3, 2.56 ppm. ^{13}C NMR: *C*H, 175.9 ppm; *C*H$_3$, 22.6 ppm. λ_{max} (ϵ_{max}): 20 000 cm^{-1} (6100).

Physical Measurements. Electronic and CD spectra of the Fe^{II} chelates in water and the Fe^{III} chelates in 1 × 10^{-3} M HCl were recorded on a Shimadzu UV-210A spectrometer and a Jasco J-40 recording polarimeter, respectively. Infrared spectra were obtained on a Jasco IRA-2 spectrophotometer using Nujol mulls. ^{1}H and ^{13}C NMR spectra of the Fe^{II} chelates in D_2O were recorded on JEOL MH-100 and FX-100 spectrometers. ^{1}H and ^{13}C NMR spectra of the Fe^{III} chelates in D_2O containing 1 × 10^{-3} M DCl were recorded with the JEOL FX-100 spectrometer. Sodium 3-(trimethylsilyl)propionate-2,2,3,3-d_4 (TSP) and 1,4-dioxane were used as internal standards for ^{1}H and ^{13}C NMR measurements, respectively.

Electrochemistry. Cyclic voltammograms of $[Fe(CN)_4(diamine)]^{2-}$ in water were recorded on a Bioanalytical Systems CV-1B voltammetry instrument in conjunction with a Riken Denshi F-3EH XY recorder at 25 °C by using a BAS MF 2020 Ag/AgCl reference electrode, a BAS MF 2013 platinum-disk working electrode, and a platinum-wire auxiliary electrode. The sample solution, containing 1 × 10^{-3} M $[Fe(CN)_4(diamine)]^{2-}$ and 0.1 M $NaClO_4$ as supporting electrolyte, was bubbled with nitrogen gas for 20 min before measurement.

Kinetics of Disproportionation of Fe^{III} Chelates under Basic Conditions. A solution of the Fe^{III} chelate, $[Fe(CN)_4(diamine)]^-$, in 1 × 10^{-3} M HCl was added to a buffer solution (borate at pH 9.1–11.3 and phosphate at pH 11.5) at 25 °C. The ionic strength of the stock solutions was adjusted to 0.3 M with sodium chloride. Formation of tetracyano(diimine)ferrate(II) from tetracyano(diamine)ferrate(III) was followed by the measurement of absorbance changes at the λ_{max} for the diimine comlex (at 500 nm for the *meso*- and *R*-bn complexes and at 517 nm for the *cis*-chxn complex) at 25 °C with a Hitachi 228 spectrometer.

Results and Discussion

The chelate rings formed by the coordination of substituted 1,2-diamines to metal ions can be divided into two groups according to the mode of substitution. The first is formed by a racemic-type 1,2-diamine and prefers a conformation with equatorial alkyl groups in both crystalline[17] and solution states[6]

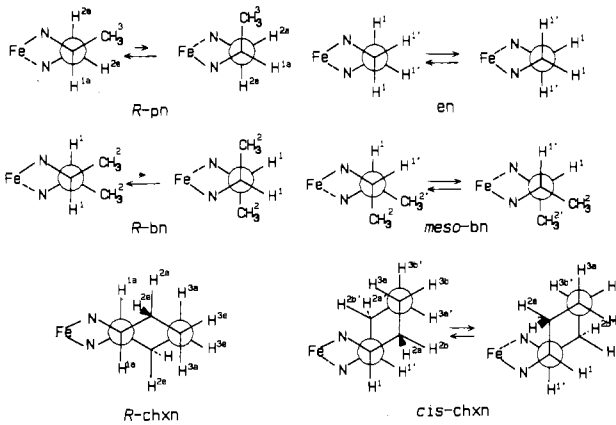

Figure 1. Schematic structures of chelates and the numbering of protons.

as shown in Figure 1. Thus the chelate rings formed by (*R*)-1,2-propanediamine (*R*-pn), *R*-bn, and *R*-chxn are predominantly in the λ conformation. The second, formed by a meso-type 1,2-diamine such as *meso*-bn and *cis*-chxn, is unsymmetric in the crystalline state as demonstrated by X-ray crystallography.[18-21] In solution, however, this class of chelate ring rapidly alternates between δ and λ conformations at ambient temperature, as shown in Figure 1, on the basis of the NMR spectra.[7,22-24] An ethanediamine chelate is regarded as belonging to the meso-type.

The tetracyanoferrate(II) complexes of *R*-bn and *meso*-bn were synthesized in a manner similar to the previous preparations:[1-4] 4 equiv of sodium cyanide was added to a methanol solution of tris(diamine)iron(II) generated in situ under a prepurified nitrogen atmosphere. The *meso*- and *R*-bn complexes showed two absorptions in the near-ultraviolet region: at 25 600 (ϵ_{max} = 439) and 32 000 cm^{-1} (ϵ_{max} = 453) and at 25 700 (ϵ_{max} = 376) and 32 000 cm^{-1} (ϵ_{max} = 422), respectively. The CD spectrum of the *R*-bn complex showed a negative and a positive Cotton effect for the first absorption band at 22 600 ($\Delta\epsilon$ = −0.22) and 26 300 cm^{-1} ($\Delta\epsilon$ = +0.32). These Cotton effects indicate that the chelate ring of *R*-bn assumes a λ conformation with both methyl groups in the equatorial position.[2]

The Fe^{III} complexes were prepared by the oxidation of the corresponding Fe^{II} complexes with hydrogen peroxide under acidic conditions. The absorption and CD spectra shown in Figure 2 are similar to those of the Fe^{III} complexes reported previously.[3] The relatively strong absorption observed in the near-ultraviolet region suggests the existence of a CN→Fe charge transfer. The Cotton effect at the longest wavelength is positive whenever the 1,2- and 1,3-diamines assume a λ conformation on coordination.[3,25]

^{1}H and ^{13}C NMR Spectra of the Tetracyanoferate(II) and Tetracyanoferrate(III) Chelates with *rac*- and *meso*-1,2-Diamines. The Fe^{II} complexes are diamagnetic, and the Fe^{III} complexes are of low spin with $(t_{2g})^5$ electronic configuration.[3] The observed as well as other relevant chemical shifts[8] are listed in Table I. Numbering for ^{1}H nuclei is denoted in Figure 1. Numberings for ^{13}C nuclei and their ^{1}H-bonded nuclei are identical. Subscripts a, b, and e denote different positions of ^{1}H bonded to the same carbon atoms.

(17) Saito, Y. *Absolute Stereochemistry of Chelate Complexes* in *Topics in Stereochemistry*; Eliel, E. L., Allinger, N. L., Eds.; Wiley: New York, 1978; Vol. 10, p 95.
(18) Ito, T.; Marumo, F.; Saito, Y. *Acta Crystallogr.* **1971**, *B27*, 1695.
(19) Gargallo, M. F.; Mather, J. D.; Duesler, E. N.; Tapscott, R. E. *Inorg. Chem.* **1983**, *22*, 2888.
(20) Lock, C. J. L.; Pilon, P. *Acta Crystallogr.* **1981**, *B37*, 45.
(21) Hollis, L. S.; Amundsen, A. R.; Stern, E. W. *J. Am. Chem. Soc.* **1985**, *107*, 274.
(22) Bagger, S. *Acta Chem. Scand.* **1974**, *A28*, 467.
(23) Erickson, L. E.; Sarneski, J. E.; Reilley, C. N. *Inorg. Chem.* **1975**, *14*, 3007.
(24) Yano, T.; Tsukada, T.; Saburi, M.; Yoshikawa, S. *Inorg. Chem.* **1978**, *17*, 2520.
(25) Goto, M.; Nakayabu, H.; Ito, H.; Tsubamoto, H.; Nakabayashi, K.; Kuroda, Y.; Sakai, T. *Inorg. Chem.* **1986**, *25*, 1684.

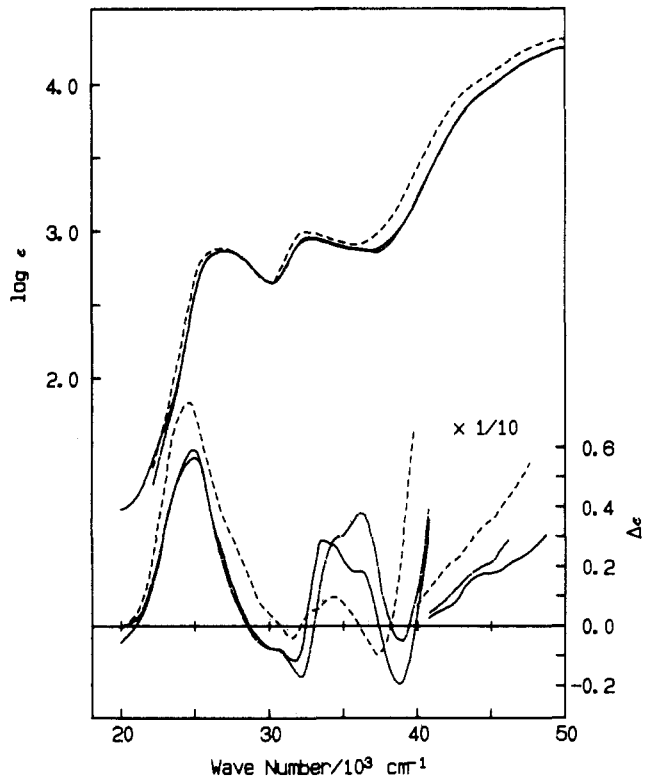

Figure 2. Electronic and CD spectra of $[Fe(CN)_4(R\text{-bn})]^-$ (—), $[Fe(CN)_4(R\text{-chxn})]^-$ (---), and $[Fe(CN)_4(R\text{-pn})]^-$ (-·-) in 1×10^{-3} M hydrochloric acid.

Table I. Chemical and Isotropic Shifts of $[Fe^{II}(CN)_4(diamine)]^{2-}$ and $[Fe^{III}(CN)_4(diamine)]^-$

diamine	nucleus[a]	chem shift/ppm[b] Fe^{II}	chem shift/ppm[b] Fe^{III}	isotropic shift/ppm[c]
meso-bn	H^1	2.91	−3.66	6.57
	H^2	1.07	3.85	2.78
	C^1	53.6	191.7	138.1
	C^2	15.9	−20.8	−36.7
R-bn	H^1	2.29	17.91	15.62
	H^2	1.17	7.36	6.19
	C^1	57.3	231.5	174.2
	C^2	20.5	−48.2	−68.7
cis-chxn	H^1	2.86	−2.62	−5.48
	H^2	1.59	2.57	0.98
			4.87	3.28
	H^3	1.48	4.87	3.39
			5.44	3.96
	C^1	55.6	191.4	135.8
	C^2	28.1	−3.3	−31.4
	C^3	22.2	26.2	4.0
R-chxn[d]	H^{1a}	2.04	15.98	13.94
	H^{2a}	1.16	10.86	9.70
	H^{2e}	2.04	10.86	8.82
	H^{3a}	1.16	6.61	5.45
	H^{3e}	1.65	1.49	−0.16
	C^1	60.6	258.3	197.7
	C^2	35.6	−18.9	−54.5
	C^3	25.3	30.0	4.7
R-pn[d]	H^{1a}	2.74	17.40	14.66
	H^{2a}	2.16	17.40	15.24
	H^{2e}	2.61	−20.05	−22.66
	H^3	1.22	9.31	8.09
	C^1	52.7	241.5	188.8
	C^2	50.9	248.0	197.1
	C^3	19.6	−49.2	−68.8
en[d]	H^1	2.50	−0.91	−3.41
	C^1	45.2	251.6	206.4

[a] For abbreviation, see text. [b] Positive values indicate downfield shifts. Internal standards are TSP (0.0 ppm) for ^1H NMR and dioxane (67.44 ppm) for ^{13}C NMR. [c] Isotropic shift is defined as the difference in chemical shift between those of the Fe^{III} and Fe^{II} complexes. [d] Reference 8.

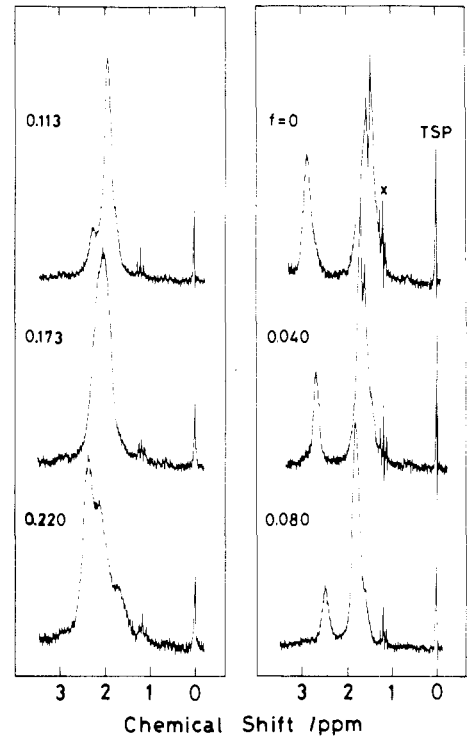

Figure 3. ^1H NMR spectral changes of the mixture of $[Fe(CN)_4(cis\text{-chxn})]^{2-}$ and $[Fe(CN)_4(cis\text{-chxn})]^-$ (f = mole fraction of the Fe^{III} complex).

Fe^{II} Complexes. The ^1H signal assignments for the Fe^{II} *R*-bn and *meso*-bn complexes are straightforward because of the intensity ratio of 1:3 for the methine and methyl protons. Observation of two peaks for the *meso*-bn complex indicates that the chelate ring rapidly changes the conformation (Figure 1) on the NMR time scale at room temperature, so that the two resonances are attributed respectively to the time-averaged methyl and methine signals. Since the C^1 shift for the *R*-bn complex is close to that for $[Fe(CN)_4(R\text{-pn})]^{2-}$, 19.6 ppm,[8] and is different by 4.6 ppm from that for the *meso*-bn complex, the *R*-bn chelate ring is predominantly in the λ conformation with two equatorial methyl groups, as expected from the CD spectrum.

The *cis*-chxn complex shows three ^{13}C resonances at room temperature. This represents the time-averaging of C^1 and $C^{1'}$, C^2 and $C^{2'}$, and C^3 and $C^{3'}$ signals by rapid conformational interconversion, as shown in Figure 1. The assignment of the ^{13}C signals is based on the fact that the ^{13}C nucleus is further from the amino group when it resonates at higher field. The *cis*-chxn complex also shows three ^1H peaks at 2.89, 1.60, and 1.49 ppm with an area ratio of 1:2:2, respectively, as shown at the top right of Figure 3. The lowest field signal is assigned to H^1 based on the area ratio. The remaining two peaks at 1.60 and 1.49 ppm are attributed to the averaged signals of $H^{2a,b}$ and $H^{3a,b}$, respectively, because these values are close to the mean of the H^{2a} and H^{2e} shifts and that of the H^{3a} and H^{3e} shifts of the Fe^{II} *R*-chxn complex: 1.60 and 1.41 ppm.[8]

The chemical shifts of H^1 and C^2 of the bn and chxn complexes are dependent on their orientation relative to the chelate ring. The H^1 peaks of the racemic-type 1,2-diamine chelates appear at higher field than those of the corresponding meso-type 1,2-diamine chelates, and their C^2 shifts are in the opposite direction. Such differences in chemical shifts are in agreement with the results of conformation analysis for Pt complexes with 2,3-butanediamines and cyclohexanediamines based on coupling constants between the Pt nucleus and H^1 and C^2 nuclei,[22,23,26] where alkyl groups of racemic-type 1,2-diamine chelates are in equatorial positions and meso-types alternate between the δ and λ conformations with one axial and one equatorial alkyl group.

(26) Lind, T.; Toftlund, H. *Acta Chem. Scand.* **1982**, *A36*, 489.

In the present Fe^{II} complexes, the C^1 shifts for the meso-type diamines are upfield from those for the racemic-type diamines. Similar trends in C^1 shift have been reported for Pt complexes of bn and chxn[22,23,26] and Co^{III} complexes of bn.[7,19] For Co^{III} complexes,[7] the chemical shift difference is explained by a steric perturbed shift, as suggested by Grant et al.[27]

Fe^{III} Complexes. The signal assignment for the *R*-bn and *meso*-bn complexes is unambiguous because of the simple intensity ratio. The *cis*-chxn complex exhibited four ^1H signals at 5.44, 4.87, 2.57, and −2.62 ppm with an area ratio of 1:2:1:1. These are assigned by using rapid electron exchange between $[Fe^{II}(CN)_4(cis\text{-chxn})]^{2-}$ and $[Fe^{III}(CN)_4(cis\text{-chxn})]^{-}$.[8] The mixture of the two complexes showed ^1H and ^{13}C signals at weighted-average positions between the two components. Therefore, the successive addition of the Fe^{III} complex to the Fe^{II} complex shifted each signal in proportion to the mole fraction of the Fe^{III} complex, as shown in Figure 3. This procedure correlates each signal of the Fe^{III} chelate to the signal of the Fe^{II} chelate, as shown in Figure 4.

The ^1H NMR spectra of $[Fe(CN)_4(R\text{-pn})]^-$ and $[Fe(CN)_4(R\text{-chxn})]^-$ are well-resolved and strongly orientation dependent.[8] The axial protons on the chelate rings of these Fe^{III} complexes resonate at ca. 16–19 ppm, while the equatorial protons resonate at ca. −12 to −20 ppm.[8] The H^1 protons of the *R*-bn complex resonate at 17.91 ppm and therefore are in axial positions relative to the chelate ring as expected from the CD spectrum.

The axial and equatorial ring protons of the Fe^{III} *meso*-diamine complexes show the time-averaged signals at −0.91 (en),[8] −3.66 (*meso*-bn), and −2.62 ppm (*cis*-chxn). These chemical shifts are close to the mean of the methylene shifts of $[Fe(CN)_4(R\text{-pn})]^-$, −1.33 ppm.[8] This fact confirms that the meso-type diamines alternate between δ and λ conformations at room temperature and that the ring protons simultaneously change their orientations between axial and equatorial in a similar manner to that of the Fe^{II} complexes. The half-line-widths of the signals increase in the order of *cis*-chxn (92 Hz) > *meso*-bn (22 Hz) > en (20 Hz) at 303 K, which reflects the difference in the rate of interconversion.[28]

The time-averaged H^2 signal of the *meso*-bn complex was observed at 3.85 ppm. Since this shift is upfield from the equatorial methyl shifts of the *R*-pn and *R*-bn complexes (9.31[8] and 7.36 ppm), the axial H^2's of the *meso*-bn chelate are expected to resonate at a higher magnetic field than the equatorial, and the estimated shift is 0.34 ppm on the basis of the observed value for the *R*-bn chelate.

The C^1 and C^2 shifts are different in the *meso*-bn and *R*-bn complexes. A similar tendency is also observed for C^1 and C^2 shifts of *cis*-chxn and *R*-chxn. The C^1 nuclei resonate at much higher field for meso-type diamines (*meso*-bn, 191.7 ppm; *cis*-chxn, 191.4 ppm) than for racemic-type diamines (*R*-bn, 231.5 ppm; *R*-chxn,[8] 258.3 ppm), whereas the C^2 nuclei show an opposite trend: *meso*-bn, −20.8 ppm; *cis*-chxn, −3.3 ppm; *R*-bn, −48.2 ppm; *R*-chxn,[8] −18.9 ppm. The reason for these differences is not clear at present.

Electrochemistry. The $E_{1/2}$ values of the four tetracyano(diamine)ferrates were measured by cyclic voltammetry. The separation of the cathode and anode peaks was narrower than 80 mV at a sweep rate of less than 10 mV s^{-1}. The alkyl substitution of ethanediamine, of which $E_{1/2}$ has been reported to be 0.303 V vs NHE,[12] results in a decrease in $E_{1/2}$. The difference in the mode of alkyl substituion has a small effect on $E_{1/2}$: 0.263, 0.259, 0.261, and 0.258 V vs NHE for the *cis*-chxn, *R*-chxn, *meso*-bn, and *R*-bn complexes, respectively.[29]

Dehydrogenation Product of Tetracyano(1,2-diamine)ferrate(II). A ligand-oxidized complex, $[Fe^{II}(CN)_4(2,3\text{-butanediimine})]^{2-}$ was prepared by oxidation of $[Fe(CN)_4(meso\text{-bn})]^{2-}$ with hydrogen peroxide under neutral conditions at 40 °C and was isolated as the 1,4-dimethyl-1,4-diazoniabicyclo[2.2.2]octane salt. A strong metal-to-ligand charge-transfer (MLCT) band characteristic of the 1,2-diimine–Fe^{II} chromophore appeared at 20 000 cm^{-1} with ϵ_{max} of 6100 M^{-1} cm^{-1}. The corresponding MLCT bands were observed at 19 340, 19 400, and 19 400 cm^{-1} for the ethanediimine, 1,2-propanediimine, and 1,2-cyclohexanediimine complexes, respectively.[3] Thus, the two adjacent methyl groups seem to modulate this chromophore so as to cause a blue shift of 600 cm^{-1}. The coordinated 2,3-butanediimine has been reported for $[Ru(NH_3)_4(2,3\text{-butanediimine})]^{2+}$, of which the MLCT band appeared at 21 500 cm^{-1} (ϵ_{max} = 7.2 × 10^3 M^{-1} cm^{-1}).[30]

Table III. Third-Order Rate Constants of Disproportionation of $[Fe^{III}(CN)_4(diamine)]^-$

diamine	k/M^{-2} s^{-1}	diamine	k/M^{-2} s^{-1}
cis-chxn	(4.62 ± 0.11) × 10^4	*R*-bn	(1.28 ± 0.29) × 10^4
R-chxn[a]	(2.82 ± 0.27) × 10^3	*R*-pn[a]	(2.06 ± 0.17) × 10^4
meso-bn	(2.34 ± 0.70) × 10^4	en[a]	(3.19 ± 0.12) × 10^4

[a] Reference 4.

Disproportionation of Fe^{III} Complexes. As described in the Introduction, the disproportionation of **2** under basic conditions yields **3** with simultaneous dehydrogenation in addition to **1**, when *R*-chxn is used as the diamine. Stoichiometry of the disproportionation was expressed with eq 1.[4] A four-electron oxidation is required for the formation of **3** from **1**. For other diamine complexes, the yield of **3** was less than 25%.[4] This low value is attributable to **4**, the production of which requires a two-electron oxidation.

Thus, the products of the disproportionations are tetracyanoferrate(II) complexes of diimine (**3**), monoimine (**4**), and diamine (**1**), as shown in eq 2. After the oxidation–reduction equivalences

$$[Fe^{III}(CN)_4(diamine)]^- + OH^- \rightarrow x[Fe^{II}(CN)_4(diimine)]^{2-} + y[Fe^{II}(CN)_4(monoimine)]^{2-} + (3x + y)[Fe^{II}(CN)_4(diamine)]^{2-} + H_2O \quad (2)$$

in eq 2 are balanced, the product distribution is x:(0.5 − 2x):(0.5 + x) for **3**, **4**, and **1**, respectively. The yield of **3** was evaluated spectrophotometrically at the MLCT absorption maximum and was found to decrease in the following order: *R*-chxn (25.0%) > *cis*-chxn (20.8%) > *R*-bn (19.6%) > *meso*-bn complex (15.8%).

a. Kinetics of the Disproportionation. The disproportionation rate of **2** was measured at 25 °C in borate or phosphate buffer with an ionic strength of 0.3 M and pH 9.1–11.5 by monitoring the increase in absorbance at 500 or 517 nm. The conversion of **2** was expressed by the ratio of the absorbance at time t, A_t, to that at infinite time, A_∞, which was measured after at least 20 half-lives. Since the reactants have no absorption at 500–517 nm, the remaining portion of **2** is $(A_\infty - A_t)/A_\infty$. In most kinetic runs, plots of $(A_t - A_0)/(A_\infty - A_t)$ against time yielded a straight line, as shown in Figure 5. The second-order rate constant, k_{obsd}, was obtained by dividing the slope with the initial concentration of **2**, and these values are summarized in Table II (supplementary material). The pH profiles of k_{obsd}, shown in Figure 6, indicate that k_{obsd} is proportional to the concentration of hydroxide ion, $[OH^-]$.

Thus, the rate of the disproportionation can be expressed with eq 3, as reported previously for this class of complexes.[4]

$$-d[Fe^{III}]/dt = k_{obsd}[Fe^{III}]^2 = k[Fe^{III}]^2[OH^-] \quad (3)$$

The third-order rate constants, k, are tabulated in Table III along with those of the *R*-chxn, *R*-pn, and en complexes reported previously.[4] A comparison of k values of the *meso*- and *rac*-diamine

(27) Grant, D. M.; Cheney, B. V. *J. Am. Chem. Soc.* **1967**, *89*, 5315.
(28) Kuroda, Y.; Tanaka, N.; Goto, M.; Sakai, T. *Inorg. Chem.* **1989**, *28*, 997.
(29) The $E_{1/2}$ values of the tetracyanoferrate(II/III) complexes of 2-(aminomethyl)pyridine, *N,N'*-dimethylethanediamine, and ethanediamine were remeasured under the same conditions as this study and found to be 401, 300, and 281 mV vs NHE. These values are lower by ca. 40 mV than those reported previously.[4]
(30) Evans, I. P.; Everett, G. W.; Sargeson, A. M. *J. Am. Chem. Soc.* **1976**, *98*, 8041.

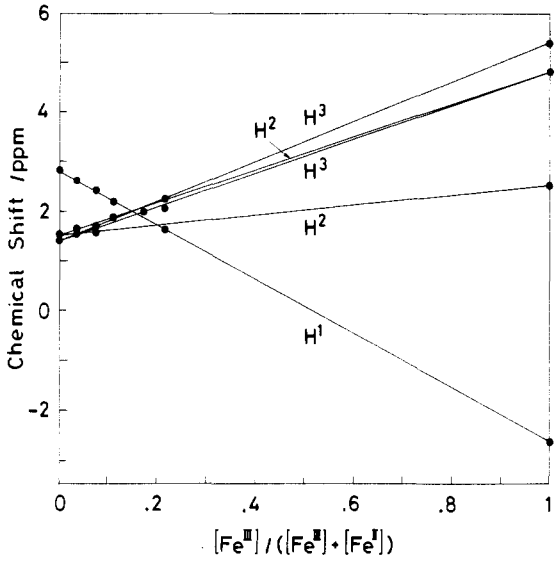

Figure 4. Plots of chemical shifts for the mixture of $[Fe(CN)_4(cis\text{-chxn})]^{2-}$ and $[Fe(CN)_4(cis\text{-chxn})]^-$ vs mole fraction of the Fe^{III} complex.

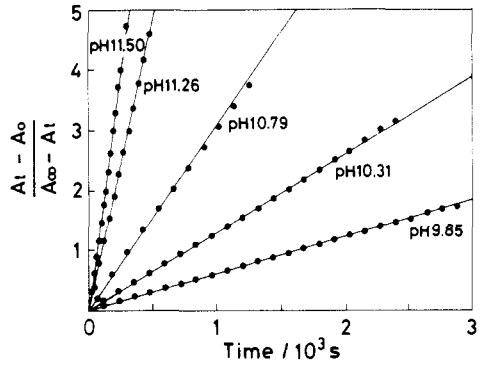

Figure 5. Second-order rate plots of the disproportionation of $[Fe^{III}(CN)_4(meso\text{-bn})]^-$.

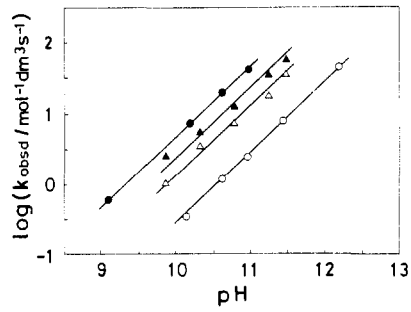

Figure 6. pH profiles of the observed second-order rate constants for the disproportionation of $[Fe^{III}(CN)_4(diamine)]^-$ with the following diamines: (●) *cis*-chxn; (○) *R*-chxn; (▲) *meso*-bn; (△) *R*-bn.

complexes reveals that the former has a larger k than the latter: *cis*-chxn:*R*-chxn = 16.4:1; *meso*-bn:*R*-bn = 1.8:1.

b. Steric Effect. The disproportionation described by eq 2 is thought to proceed in three steps:[4]

$$2[Fe^{III}(CN)_4(diamine)]^- + 2OH^- \xrightarrow{k_4} [Fe^{II}(CN)_4(monoimine)]^{2-} + [Fe^{II}(CN)_4(diamine)]^{2-} + 2H_2O \quad (4)$$

$$[Fe^{II}(CN)_4(monoimine)]^{2-} + [Fe^{III}(CN)_4(diamine)]^- \rightleftarrows [Fe^{III}(CN)_4(monoimine)]^- + [Fe^{II}(CN)_4(diamine)]^{2-} \quad (5)$$

$$[Fe^{III}(CN)_4(monoimine)]^- + [Fe^{III}(CN)_4(diamine)]^- + 2OH^- \xrightarrow{k_6} [Fe^{II}(CN)_4(diimine)]^{2-} + [Fe^{II}(CN)_4(diamine)]^{2-} + 2H_2O \quad (6)$$

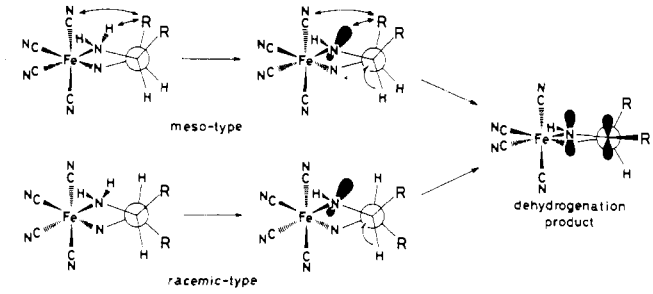

Figure 7. Stereochemistry of the starting complex and the deprotonated intermediate involved in the first and rate-determining steps of the dehydrogenation.

Prior to the dehydrogenation of **4**, this complex must be oxidized to the Fe^{III} complex by the electron exchange of eq 5. This electron exchange is expected to be rapid because the species in eq 5 are in a low-spin state.[2] However, the $E_{1/2}$ values for the two monoimine complexes are expected to be higher than those for the diamine complexes.[31] The concentration of $[Fe^{III}(CN)_4(monoimine)]^-$ should, therefore, be kept low during the course of the reaction. The fact that **3** was the main dehydrogenated product of the disproportionation of **2** requires that k_6 be much larger than k_4. Reaction 6 should be less susceptible to diamine variation than reaction 4 because the monoimine complexes obtained from both of the *meso*- and *rac*-diamine complexes are identical, i.e., **2a** and **2b**. Thus, the product distribution reflects the relative magnitude of k_4 vs k_6. The smaller k_4 results in the larger yield of **3**. This is in agreement with the order observed for the rate constant and the yield of **3**. Therefore, the rate constant of the overall reaction and the yield of **3** are governed by reaction 4.

X-ray diffraction analyses for Co^{III},[19,32,33] Pd^{II},[18] and Pt^{II} complexes[20,34] of the meso-type and racemic-type 1,2-diamines have revealed that both dihedral angles of the N–C–C–N and C–C–C–C moieties for the *meso*-diamine chelates are smaller than those for the corresponding *rac*-diamines. These results indicate that the *meso*-diamine chelates have more flattened conformations, i.e., greater ring strain, compared with those of the *rac*-diamine chelates. This increment in ring strain is attributable to the nonbonded interaction between the axial alkyl groups and the apical ligand and/or hydrogen atoms within the chelate, as shown at the left side of Figure 7. Thus, the *meso*-bn and *cis*-chxn chelates are expected to have strain energy greater than that of the *R*-bn and *R*-chxn chelates. Although there is no repulsion between adjacent methyl groups in the *cis*-chxn complex present in the *meso*-bn chelate, the former chelate is considered to have greater repulsion between the methylene and amino hydrogens and/or the cyanide ions compared with the repulsion energy in the *meso*-bn complex due to the two methyl groups.

Equation 3 leads to the assumption, which has been proposed previously,[4] that the intermediate governing the dehydrogenation is **2** deprotonated at the amino group or its one-electron-oxidized form shown at the center of Figure 7. This intermediate is expected to have a pseudo planar trigonal structure at the deprotonated nitrogen center. Since steric repulsion due to the meso-type 1,2-diamine will be released on formation of this intermediate, the stabilization energy obtained in this process is presumed to be greater for the meso-type chelate than for the racemic-type: *cis*-chxn > *R*-chxn, *meso*-bn > *R*-bn, *cis*-chxn > *meso*-bn. This order is in agreement with that observed in the rate constant, k. The difference in k, therefore, can be explained by this stabili-

(31) The $E_{1/2}$ value of the monoimine complex is not available. But the $E_{1/2}$ value of the 2-(aminomethyl)pyridine complex, which can be classified as a monoimine complex, is substantially higher than those of the diamine complexes (ref 4). Furthermore, Busch et al. reported that the introduction of an imine group into a macrocyclic poly(amine)iron(II) complex raises the $E_{1/2}$ value by 49 mV: Lovecchio, F. V.; Gore, E. S.; Busch, D. H. *J. Am. Chem. Soc.* **1974**, *96*, 3109.

(32) Kobayashi, A.; Marumo, F.; Saito, Y. *Acta Crystallogr.* **1983**, *C39*, 807.
(33) Duesler, E. N.; Gargallo, M. F.; Tapscott, R. E. *Acta Crystallogr.* **1982**, *B38*, 1300.
(34) Larsen, K. P.; Toftlund, H. *Acta Chem. Scand.* **1977**, *A31*, 182.

zation.

Acknowledgment. This work was partially supported by a Grant-in-Aid for Scientific Research (No. 61540452) from the Ministry of Education, Science, and Culture of Japan.

Supplementary Material Available: Table II, listing kinetic results of the disproportion of $[Fe^{III}(CN)_4(diamine)]^-$, where diamine = (1*R*,2*S*)-*cis*-cyclohexanediamine (*cis*-chxn), (2*R*,3*S*)-butanediamine (*meso*-bn), and (2*R*,3*R*)-butanediamine (*R*-bn) (1 page). Ordering information is given on any current masthead page.

Contribution from the Department of Chemistry,
The University of Michigan, Ann Arbor, Michigan 48109

Synthesis, Structural Characterization, and Properties of the $[Mo_2O_2S_9]^{2-}$ Thio Anion and the $[Mo_4O_4S_{18}]^{2-}$, $[Mo_2O_2S_8(SCH_3)]^-$, and $[Mo_2O_2S_8Cl]^-$ Derivatives

A. I. Hadjikyriacou and D. Coucouvanis*

Received November 17, 1988

Investigation of the oxidative transformations of $[MoOS_8]^{2-}$ has led to the characterization of the Mo(VI) oxo disulfido complexes $[Mo_2O_2S_9]^{2-}$ and $[Mo_2O_2S_{10}]^{2-}$ as a solid mixture in the structure of $(Et_4N)_2[Mo_2O_2S_{9.14}]$ (I). Oxidative coupling of I affords the Mo(VI) linear tetramer $(Et_4N)_2[Mo_4O_4S_{18}]$ (III). Reaction of either I or III with $NiCl_2$ in MeCN generates the new chloro derivative $(Et_4N)[Mo_2O_2S_8Cl]$ (IV) as a result of ligand exchange. The nucleophilicity of $[Mo_2O_2S_9]^{2-}$ is demonstrated in its reaction with MeI, which gives the methanethiolato-bridged derivative $(Et_4N)[Mo_2O_2S_8(SMe)]$ (II). Both I and II crystallize in the space group $P2_1/c$ with four molecules per unit cell. The cell dimensions are a = 16.734 (2) Å, b = 10.407 (2) Å, c = 17.457 (3) Å, and β = 97.06 (1)° for I and a = 13.866 (4) Å, b = 12.927 (4) Å, c = 14.219 (4) Å, and β = 118.80 (2)° for II. Compounds III and IV crystallize in space groups $P\bar{1}$ and $P2_1/n$, respectively. The cell dimensions are a = 11.726 (3) Å, b = 12.851 (3) Å, c = 16.183 (4) Å, α = 79.21 (2)°, β = 82.68 (2)°, and γ = 79.65 (2)° for III and a = 13.309 (5) Å, b = 10.663 (3) Å, c = 16.360 (5) Å, and β = 113.74 (2)° for IV. Full-matrix refinement of 257 parameters on 3065 data for I, 208 parameters on 1803 data for II, 357 parameters on 5094 data for III, and 163 parameters on 1478 data for IV gave final R_w values of 0.064, 0.033, 0.052, and 0.037, respectively. The structures of I–IV contain Mo(VI) ions with pseudo-pentagonal-bipyramidal environments. One of the axial sites is occupied by a terminal oxo ligand. The second one is occupied by an intramolecularly weakly interacting sulfur. Two η^2-S_2^{2-} ligands and a bridging sulfur ligand define the equatorial plane of the pentagonal bipyramid. Adjacent bipyramids share the bridging ligand as common equatorial site: S^{2-} in $[Mo_2O_2S_9]^{2-}$, η^1,η^1-S_2^{2-} in $[Mo_2O_2S_{10}]^{2-}$, SMe^- in $[Mo_2O_2S_8(SMe)]^-$, η^2,η^1-S_2^{2-} in $[Mo_2O_2S_8Cl]^-$, and one η^1,η^1-S_2^{2-} and two η^2,η^1-S_2^{2-} ligands in $[Mo_4O_4S_{18}]^{2-}$. Selected bond lengths (Å): in I, Mo–Mo = 3.606 (1), Mo=O = 1.676 (6); in II, Mo–Mo = 3.570 (1), Mo–SMe = 2.525 (2), Mo=O = 1.672 (6); in III, Mo–Mo = 3.606 (1) and 3.561 (1), Mo=O = 1.676 (8), Mo–η^1,η^1-S_2 = 2.417 (3); in IV, Mo–Mo = 3.550 (1), Mo=O = 1.654, Mo–Cl = 2.388 (3). The spectroscopic properties as well as detailed synthetic procedures for I–IV are reported.

Introduction

A large body of structural and reactivity studies in molybdenum–sulfur chemistry has grown in recent years. This interest derives mainly from (a) the apparent importance of Mo–S coordination in the function of certain molybdenum-containing enzymes[1] and (b) the reactivity characteristics of "sulfided" molybdenum in the catalysis of the industrially important hydrodesulfurization (HDS) reaction.[2]

Extensive investigations in the reactivity of the tetrathiomolybdate anion, $[MoS_4]^{2-}$, have established its versatility as a bidentate ligand in the formation of heteronuclear transition-metal sulfides of the type $[M'(MoS_4)_2]^{3-}$ (M' = Co, Fe),[3] $[M'(MoS_4)_2]^{2-}$ (M' = Zn, Ni, Fe, Co, Pd, Pt),[4] and $[L_2Fe(MoS_4)]^{2-}$.[5] Further explorations in the chemistry of $[MoS_4]^{2-}$ has led to the discovery of a family of soluble binary molybdenum sulfides, $Mo_xS_y^{2-}$, that includes $[(S_4)_2MoS]^{2-}$,[6] $[(S_4)MoS(MoS_4)]^{2-}$,[7] $[(MoS_4)_2MoS]^{2-}$,[8] $[(S)_2Mo(\mu\text{-}S)]_2^{2-}$,[7] $[(S)_2Mo(\mu\text{-}S)_2MoS(\eta^2\text{-}S_2)]^{2-}$,[7] $[(\eta^2\text{-}S_2)SMo(\mu\text{-}S)]_2^{2-}$,[9] $[(\eta^2\text{-}S_2)SMo(\mu\text{-}S)_2MoS(S_4)]^{2-}$,[6,10] $[(S_4)SMo(\mu\text{-}S)]_2^{2-}$,[6,11] $[(\eta^2\text{-}S_2)_2Mo(\mu\text{-}\eta^2,\eta^2\text{-}S_2)]_2^{2-}$,[12] and $[Mo_3(\mu\text{-}S)(\mu\text{-}\eta^2,\eta^2\text{-}S_2)_3(\eta^2\text{-}S_2)_3]^{2-}$.[13]

The unique reactivity characteristics of the Mo-coordinated S_2^{2-} and S_4^{2-} ligands, toward activated alkynes or CS_2, have been explored in some detail. The reactions of dicarbalkoxyacetylenes with the S_x^{2-} ligands[14] depend on the proximal terminal ligand (O or S) attached to the Mo atom.

The reactions of the O=Mo(S_x) units in either $[(\eta^2\text{-}S_2)OMo(\mu\text{-}S)]_2^{2-}$[14b] or $[(\eta^2\text{-}S_2)OMo(\mu\text{-}S)_2MoO(S_4)]^{2-}$[14c] give rise to derivatives that contain vinyl disulfido ligands formed by the apparent insertion of the alkyne into the Mo–S_x bond. In contrast, similar reactions with the S=Mo(S_x) units in $[(S_4)_2MoS]^{2-}$ or $[(\eta^2\text{-}S_2)SMo(\mu\text{-}S)_2MoS(S_4)]^{2-}$ result in the conversion of the S_x^{2-} ligands to dithiolenes. The latter can be described formally as the result of cycloaddition to the Mo-coordinated S_x^{2-} ligands.

(1) (a) Cramer, S. P.; Stiefel, E. I. In *Molybdenum Enzymes*; Spiro, T., Ed.; Wiley: New York, 1985. (b) *Molybdenum and Molybdenum Containing Enzymes*; Coughlan, M. P., Ed.; Pergamon Press: New York, 1980.

(2) (a) Massoth, F. E. *Adv. Catal.* **1978**, *27*, 265. (b) Töpsoe, J.; Clausen, B. S. *Catal. Rev.—Sci. Eng.* **1984**, *26*, 395. (c) Weisser, O.; Landa, S. *Sulfide Catalysts: Their Properties and Applications*; Pergamon Press: London, 1973.

(3) (a) Coucouvanis, D.; Simhon, E. D.; Baenziger, N. C. *J. Am. Chem. Soc.* **1980**, *102*, 6644. (b) McDonald, J. W.; Friesen, G. D.; Newton, W. E. *Inorg. Chim. Acta.* **1980**, *46*, L79. (c) Müller, A.; Hellmann, W.; Romer, C.; Romer, M.; Bogge, H.; Jostes, R.; Schimanski, U. *Inorg. Chim. Acta* **1984**, *83*, L75. (d) Pan, W. H.; McKenna, S. T.; Chianelli, R. R.; Halbert, T. R.; Hutchings, L. L.; Stiefel, E. I. *Inorg. Chim. Acta* **1985**, *97*, L17.

(4) (a) Müller, A.; Diemann, F.; Jostes, R.; Bogge, H. *Angew. Chem., Int. Ed. Engl.* **1981**, *20*, 934. (b) Callahan, K. P.; Piliero, P. A. *Inorg. Chem.* **1980**, *19*, 2609.

(5) (a) Coucouvanis, D.; Stremple, P.; Simhon, E. D.; Swenson, D.; Baenziger, N. C.; Draganjac, M.; Chan, L. T.; Simopoulos, A.; Papaefthymiou, V.; Kostikas, A.; Petrouleas, V. *Inorg. Chem.* **1983**, *22*, 293–308. (b) Coucouvanis, D.; Baenziger, N. C.; Simhon, E. D.; Stremple, P.; Swenson, D.; Kostikas, A.; Simopoulos, A.; Petrouleas, V.; Papaefthymiou, V. *J. Am. Chem. Soc.* **1980**, *102*, 1730. (c) Coucouvanis, D.; Simhon, E. D.; Stremple, P.; Ryan, M.; Swenson, D.; Baenziger, N. C.; Simopoulos, A.; Papaefthymiou, V.; Kostikas, A.; Petrouleas, V. *Inorg. Chem.* **1984**, *23*, 741–749. (d) Coucouvanis, D. *Acc. Chem. Res.* **1981**, *14*, 201.

(6) (a) Draganjac, M.; Simhon, E.; Chan, L. T.; Kanatzidis, M.; Baenziger, N. C.; Coucouvanis, D. *Inorg. Chem.* **1982**, *21*, 3321.

(7) Hadjikyriacou, A.; Coucouvanis, D. *Inorg. Chem.* **1987**, *26*, 2400.

(8) Pan, W. H.; Leonowicz, M. E.; Stiefel, E. I. *Inorg. Chem.* **1983**, *22*, 672.

(9) (a) Miller, K. F.; Bruce, A. E.; Corbin, J. L.; Wherland, S.; Stiefel, E. I. *J. Am. Chem. Soc.* **1980**, *102*, 5102. (b) Pan, W. H.; Harmer, M. A.; Halbert, T. R.; Stiefel, E. I. *J. Am. Chem. Soc.* **1984**, *106*, 459.

(10) Clegg, W.; Christou, G.; Garner, C. D.; Sheldrick, G. M. *Inorg. Chem.* **1981**, *20*, 1562.

(11) Cohen, A.; Christou, G.; Garner, C. D.; Sheldrick, G. M. *Inorg. Chem.* **1985**, *24*, 4657.

(12) Müller, A.; Nolte, W. O.; Krebs, B. *Inorg. Chem.* **1980**, *19*, 2835.

(13) Müller, A.; Bhattacharyya, R. G.; Pfefferkorn, B. *Chem. Ber.* **1979**, *112*, 778.

(14) (a) Draganjac, M.; Coucouvanis, D. *J. Am. Chem. Soc.* **1983**, *105*, 139. (b) Halbert, T. R.; Pan, W. H.; Stiefel, E. I. *J. Am. Chem. Soc.* **1983**, *105*, 5476. (c) Coucouvanis, D.; Hadjikyriacou, A.; Draganjac, M.; Kanatzidis, M. G.; Ileperuma, O. *Polyhedron* **1986**, *5*, 349.

0020-1669/89/1328-2169$01.50/0